
Octanol-water partition coefficients of highly hydrophobic photodynamic therapy drugs: a computational study

Roger Estrada-Tejedor*, Noemí Sabaté, Francesc Broto and Santi Nonell
Institut Químic de Sarrià, Universitat Ramon Llull, Via Augusta 390, 08017 Barcelona, Spain.

*To whom correspondence should be addressed at: Grup d'Enginyeria Molecular, Institut Químic de Sarrià (IQS), Universitat Ramon Llull, Via Augusta 390, 08017-Barcelona, Spain, telephone +34 932 672 000, fax +34 932 056 266, e-mail: roger.estrada@iqs.url.edu

Coefficient de partició octanol-aigua de fàrmacs altament hidrofòbics emprats en teràpia fotodinàmica: un estudi computacional

Coefficiente de partición octanol-agua de fármacos altamente hidrofóbicos usados en terapia fotodinámica: un estudio computacional

Recibido: 9 de abril de 2013; revisado: 2 de agosto de 2013; aceptado: 2 de agosto de 2013

RESUMEN

La terapia fotodinámica se propone como un nuevo tratamiento para tumores sólidos, basado en la inducción de la muerte celular de manera selectiva por medio de la formación de sustancias reactivas del oxígeno (citotóxicas) en los tejidos neoplásicos. La fotosensibilización del oxígeno se promueve como consecuencia de la activación (mediante luz) de un fotosensibilizador, el cual se distribuye preferentemente en el tejido de interés mediante el transporte celular. La hidrofobicidad (expresada como el logaritmo de partición octanol/agua, logP), es un factor clave en estos procesos. Aun así, no se dispone de un método computacional que permita predecir de manera inequívoca el valor de logP para fotosensibilizadores altamente hidrofóbicos. En el presente estudio se compara el uso de 12 metodologías para la predicción del valor de logP de derivados tetrapirrólicos. Además, la correlación del valor de logP con medidas experimentales de HPLC (log(k')), pone de manifiesto la posibilidad que estos dos parámetros (log(k') y logP) presenten un modelo de regresión sigmoidea.

Palabras clave: Terapia fotodinámica; fotosensibilizadores; HPLC; logP.

SUMMARY

Photodynamic therapy is a novel treatment for solid tumors based on the selective induction of cell death by the generation of cytotoxic reactive oxygen species within neoplastic tissues. Oxygen photosensitization is promoted as a consequence of the activation (using light) of a photosensitizer, which must reach the desired tissue by cellular transport. Hydrophobicity (expressed as the logarithm of octanol/water partition coefficient, logP), becomes a key factor in these processes. Unfortunately, there is no

computational method to unambiguously predict the logP value for high hydrophobic photosensitizers. In this study, a total of 12 computational methods have been tested for predicting the logP value of tetrapyrrolic derivatives. Furthermore, in the attempt to correlate logP with experimental HPLC measurements (log(k')), validation of the results leads to the proposal of a sigmoidal regression for the two parameters (log(k') and logP).

Keywords: Photodynamic therapy; photosensitizers; HPLC; logP.

RESUM

La teràpia fotodinàmica ha esdevingut un nou tractament per a tumors sòlids, basat en la inducció de la mort cel·lular de manera selectiva per mitjà de la formació de substàncies reactivas de l'oxigen (citotòxiques) en els teixits neoplàsics. La fotosensibilització de l'oxigen es promou com a conseqüència de l'activació (mitjançant llum) d'un fotosensibilitzador, el qual es distribueix preferentment en el teixit d'interès mitjançant el transport cel·lular. La hidrofobicitat (expressada com el logaritme de partició octanol/aigua, logP), esdevé un factor clau en aquests processos. Malauradament, no es disposa d'un mètode computacional que permeti predir de manera inequívoca el valor de logP per a fotosensibilitzadors altament hidrofòbics. En el present estudi es compara l'ús de 12 metodologies per a la predicció del valor de logP de derivats tetrapirròlics. A més, la correlació del valor de logP amb mesures experimentals d'HPLC (log(k')), posa de manifest la possibilitat que aquests dos paràmetres (log(k') i logP) presentin un model de regressió sigmoïdal.

Paraules clau: Teràpia fotodinàmica; fotosensibilitzadors; HPLC; logP.

INTRODUCTION

In recent years photodynamic therapy (PDT) has emerged as an alternative treatment for solid tumors (e.g., glioblastomas or carcinomas [1]) and, more recently, for other non-oncological indications such as microbial infections [2-4]. PDT is leaned on the selective destruction of tumor tissues through the local phototoxicity produced by the combination of visible light, molecular oxygen and a photoactivatable drug referred to as the photosensitizer (PS). The PS absorbs light energy and uses it to generate reactive oxygen species (ROS), particularly singlet oxygen (1O_2), the dioxygen molecule in its first electronic excited state. The ROS readily react with sensitive biomolecules, producing cellular damage which finally leads to cell death via necrosis, apoptosis or autophagy mechanisms [5-9].

The participation of light contributes to the selectivity of the therapy, conferring a key advantage since only irradiated tissues are destroyed. As in chemotherapy, a fundamental aspect of PDT is that the PS must reach the neoplastic region after its administration and accumulate there. Moreover, biochemical results demonstrate the importance of subcellular localization of the PS in the overall photodynamic efficiency [9-11] and in the extension of the cellular response [7, 12, 13]. Transport and localization are strongly bound to the hydrophobicity of the drug. The logarithm of octanol/water partition coefficient ($\log P$) is usually considered a key factor not only in the establishment of Quantitative Structure-Activity Relationships (QSAR) models for the prediction of the activity of different PS families [14-20], but also in the study of intra/extracellular transport processes which are intimately related to the final subcellular localization of the PS [21-23].

QSAR and QSPR (Quantitative Structure-Property Relationships) methods try to establish a mathematical relationship between molecular descriptors, usually derived from the chemical structure, and one or more molecular properties (i.e. molecular descriptors). Since $\log P$ can be predicted computationally, it can be included in prediction models as a molecular descriptor. Over the years, a considerable number of mathematical definitions have been proposed to calculate molecular $\log P$ from chemical structure, leading in most cases different results and fostering the ambiguity related to which method should be applied. Interestingly, $\log P$ value linearly correlates with the retention time and the logarithm of capacity factor (k') of compounds measured by HPLC [24, 25]. Thus, validation of $\log P$ prediction models should be addressed indirectly according to QSRR (Quantitative Structure-Retention Relationships) methods, which try to correlate the chemical structure of a training set with chromatographic retention time.

In this report available computational $\log P$ prediction methods are evaluated for the study of highly hydrophobic tetrapyrrolic photosensitizers (i.e. porphyrin and porphyrane derivatives) in an attempt to identify the most suitable method. As no experimental $\log P$ values are available for such hydrophobic compounds, the models were validated and ranked using experimental chromatographic retention time ($\log(k')$) values.

COMPUTATIONAL DETAILS

The logarithm of the octanol/water partition coefficient ($\log P$) can be computationally estimated by several meth-

ods, which can be classified according to their theory level [26, 27].

Constructivistic methods were proposed by Fujita et al. [28], where $\log P$ is calculated from the experimental $\log P$ value of a known molecule, used as a template (*scaffold*), which is successively substituted until the desired molecule is obtained. Each molecular change has an associated corrector factor which affects the $\log P$ value of the whole molecule.

Atomic contribution methods were firstly proposed by Broto et al. [29] and later developed by Crippen [14], in these methods each atom contributes additively to the molecular $\log P$ calculation. Thus, the obtained result is highly dependent on the atom type parameterization. Some commercial software algorithms follow this strategy, for example: SlogP and $\log P(o/w)$ implemented in MOE [30], ALOGP [31] or Actelion's AClogP definition.

In the same way, the **fragment-based methods** developed in 1973 by Rekker et al. split the molecule into its constitutive fragments. Each fragment has associated a statistically $\log P$ contribution (*fragmental constant*) and a correction factor. COSMOFrag [32] and miLOGP (developed by Molinspiration Chemoinformatics) are examples of this algorithm.

Quantum methods permit to evaluate properties directly related to $\log P$ calculation (e.g. free energy of solvation in different solvents) from chemical structure and relate them to three dimensional geometry and molecular electronic structure.

Mixed methods predict the molecular $\log P$ value applying QSAR-based algorithms which involve the calculation of other kind of molecular descriptors [33], e.g. MLOGP, ALOGPs [34], XLOGP2 and XLOGP3 [25]. Finally, there exist other algorithms (as KowWin) based on the combination of two or more of the previous methods.

The existence of such variety of prediction methods demonstrate the inherent difficulty associated to $\log P$ calculation. Furthermore, the values predicted by different methods are widely scattered in the case of very hydrophobic molecules (like tetrapyrrolic PS), because these methods were usually validated with databases of small molecules [35]. A total of 12 methods have been selected for this comparative study (Table 1), based on both their availability and reported previous experience using them [33, 36, 37]: SlogP and $\log P(o/w)$ were calculated by MOE [30] software and MLOGP, AC LogP, AB/LogP, COSMOFrag, miLOGP, KowWin, XLOGP2, XLOGP3, ALOGP and ALOGPs were calculated using ALOGPs 2.1 software [38, 39].

Table 1. Brief description of $\log P$ prediction methods used in this study.

Method	Description
$\log P(o/w)$	Linear atom type model developed from the analysis of 1827 molecules (including implicit hydrogens).
SlogP	Atomic contribution model developed by Crippen et. al. [40] using 7000 molecular structures with the correct protonated state as training set.
MLOGP	Moriguchi octanol-water partition coefficient (MLOGP) is based on quantitative structure- $\log P$ relationships, by using topological indexes [41].
AC LogP	Atom-additive method considering 369 atom-type based contribution values, obtained from 5000 molecules [42].

AB/LogP	Fragmental method based on the application of averaged correction factors, obtained from both simple and complex compounds (473 group contributions and 1076 clusters of correction factors) [43].
COSMOFrag	Calculates solvent contact interactions from polarization charge density (σ) on molecular surface. σ is estimated from precalculated profiles of a 40000 molecules database [32].
miLOGP	Based on group contributions, miLOGP identifies a total of 220 molecular fragments which include charge interactions and organometallic compounds.
KowWin	Atom/fragment contribution method. Predicted logP values are obtained starting from the measured logP of structural analogues [44].
XLOGP2	Additive atom/group model which uses 90 basic atom types [25].
XLOGP3	Knowledge-based approach based on additive atom/group model which starts from the known logP value of a similarly reference compound [25].
ALOGP	Classical atomic contribution approach which can be applied on neutral organic compounds containing C, H, O, N, S, Se, P, B, Si and halogen atoms [31,45]
ALOGPs	Self-learning method based on the use of associative neural networks to predict the logP value from the molecular structure [46].

EXPERIMENTAL

The results of the computational study were compared to experimental chromatographic retention times. Sample analyses were carried out using an HP 1200 HPLC liquid chromatograph coupled with an UV/vis dual-wavelength absorbance detector. The used chromatographic column was an XTerra™ RP18 4.6mm x 250mm 5mm particle size (Waters Technologies Corporation, USA) and the solvent used was acetonitrile/water/2-propanol (65:17.5:17.5). The chromatographic methodology was based on the Organisation for Economic Co-operation and Development (OECD) guidelines [47], using for a set of five small molecules with known logP values for calibration (Figure 1).

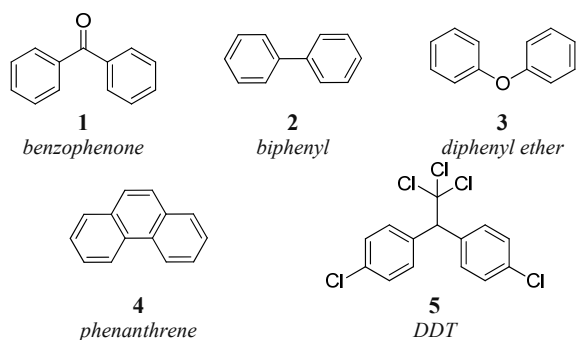


Figure 1. Molecular structure and logP values for the reference compounds used for calibration according to the OECD guideline

The applicability range of OECD regression is limited to logP values between 3 and 6.5 units and its use on high hydrophobic PS requires an extrapolation [31, 48] that must be validated. A set of 14 porphyrin and porphycene derivatives (Figure 2) was selected according to their availability and analyzed by HPLC according to OECD guidelines.

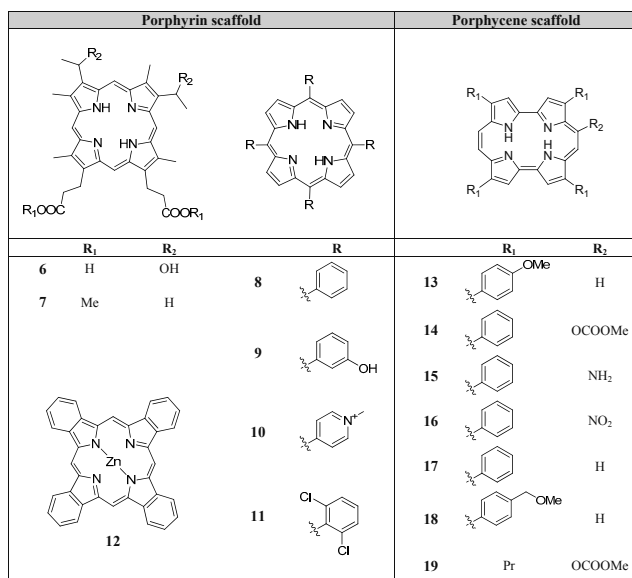


Figure 2. Molecular structure of porphyrin and porphycene derivatives

RESULTS AND DISCUSSION

The available computational methods were applied for the prediction of logP values for the OECD reference compounds and for the selected hydrophobic PSs. They are collected in Tables 2 and 3, respectively, along with the experimental chromatographic retention parameter $\log(k')$.

Table 2. Experimental and calculated data for the OECD compounds. Predicted logP values are named according to the computational method used. R^2 and Spearman's (ρ) correlation coefficients are calculated for each prediction method in contrast to logP experimental values.

	1	2	3	4	5	R^2	ρ
$\log(k')_{exp}$	0.003	0.073	0.090	0.175	0.307	-	-
$\log P_{exp}$	3.2	4.0	4.2	4.5	6.5	-	-
AB/LogP	2.9	3.9	3.4	4.5	6.6	0.95	0.9
AC LogP	3.3	3.7	3.4	3.9	6.9	0.92	0.9
ALOGP	3.2	3.4	3.4	3.4	6.3	0.97	0.7
ALOGPs	3.0	4.0	3.7	4.4	6.3	0.97	0.9
COSMOFrag	2.9	3.8	3.9	3.5	6.1	0.94	0.7
KowWin	3.2	3.8	4.1	4.4	6.8	0.99	1.0
$\log P (o/w)$	3.4	3.9	3.5	4.4	6.5	0.93	0.9
miLogP	3.4	3.7	3.7	3.6	6.7	0.89	0.6
MLOGP	3.6	3.9	3.4	4.2	6.2	0.88	0.7
SlogP	2.9	3.4	3.5	3.4	6.5	0.93	0.9
XLOGP2	3.6	3.9	3.5	4.3	6.7	0.90	0.7
XLOGP3	3.4	4.0	4.2	3.9	6.9	0.94	0.7

Table 3. Experimental and calculated data for the studied porphyrin and porphycene derivatives.

	6	7	8	9	10	11	12	13	14	15	16	17	18	19
$\log(k')_{\text{exp}}$	0.14	0.64	1.36	0.47	0.32	1.25	1.19	1.40	0.95	1.21	1.39	1.51	1.24	1.33
AB/LogP	1.3	5.8	8.8	6.3	-	10.0	-	10.0	9.6	10.0	9.2	10.0	8.8	8.9
AC LogP	3.3	6.2	7.6	6.4	2.7	12.5	7.6	7.1	8.1	7.1	7.3	7.5	6.8	7.6
ALOGP	6.7	9.5	11.2	10.2	7.1	16.5	-	11.1	10.9	10.4	11.1	11.2	10.4	10.7
ALOGPs	2.7	5.5	8.0	6.8	6.8	10.1	4.6	7.8	7.9	7.3	7.5	8.2	7.6	7.3
COSMOFrag	4.3	8.8	11.6	8.5	-	14.5	-	12.4	12.0	11.1	11.4	11.4	14.8	11.1
KowWin	4.4	11.4	11.5	9.5	8.9	16.6	8.8	11.8	11.1	10.1	10.7	11.5	10.6	10.6
$\log P$ (o/w)	4.3	6.5	11.0	9.9	9.6	15.7	5.6	11.5	11.7	11.0	11.7	11.7	12.0	8.7
miLogP	5.5	8.6	9.6	9.1	6.5	10.2	7.0	9.7	9.5	9.5	9.6	9.6	9.6	9.2
MLOGP	1.3	3.1	5.3	3.3	2.2	7.6	-	3.9	5.1	4.8	5.3	5.3	3.5	4.0
SlogP	3.9	5.5	7.6	6.5	4.4	12.9	5.6	8.6	8.5	7.9	8.2	8.6	10.3	6.5
XLOGP2	0.9	3.5	9.5	7.8	4.3	14.4	7.1	9.1	9.6	9.0	9.7	9.5	8.3	6.7
XLOGP3	2.1	5.3	10.4	9.0	6.7	15.4	6.4	9.4	9.3	8.8	9.3	9.5	8.1	8.4

Some values are missing on Table 3 for AB/LogP, ALOGP, COSMOFrag and MLOGP methods. The presence of formal charges or transition metals (e.g. in compounds **10** and **12**) means an important limitation for these fragment-based or constructivistic methods, due to the lack of parameterization resulting from the nature of the training set (most of them did not include this kind of systems). Statistical analysis for each computational method allowed evaluating the correlation between predicted $\log P$ for compounds **6-19** and their experimental $\log(k')$ values. Interestingly, compound **11** stands out as an outlier in all regressions likely as a result of specific molecular interactions with the chromatographic system. Compound **11** was therefore eliminated from the analyses.

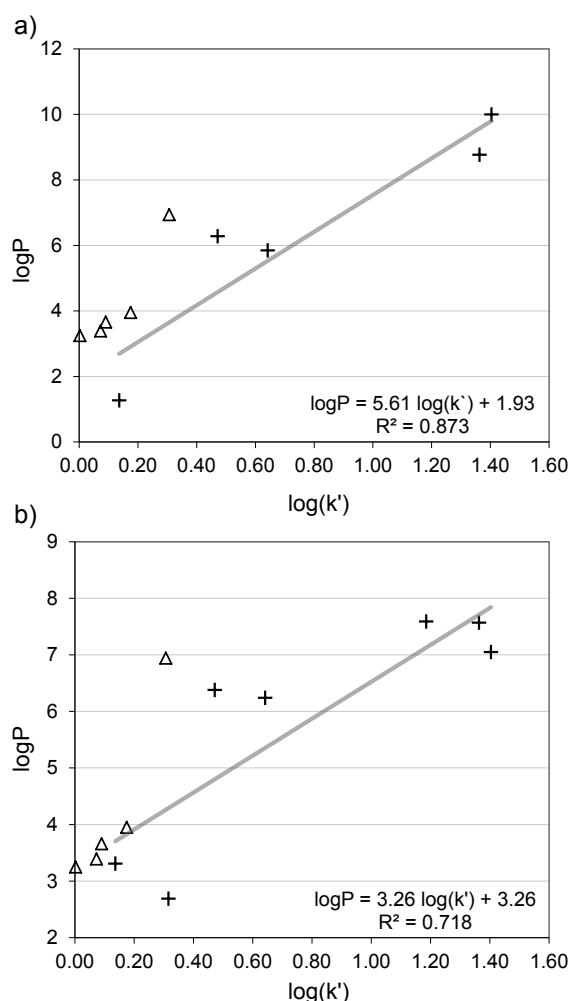
Statistical results for the training and test sets are collected on Table 4. Unfortunately, fragmental-based methods show high variability (due to fragment parameterization) and require the removal of some molecules from the training set to achieve a significant correlation. The best regression models were obtained using AC LogP, AB/LogP, COSMOFrag, and MLOGP.

Table 4. Statistical parameters derived from linear regressions of predicted $\log P$ values with experimental $\log(k')$.

Fisher's test p -value and R^2 correlation coefficient are calculated for the training set and Q^2 and Spearman's (ρ) correlation coefficients for the test set. Molecules of the training set considered as outliers (out) are indicated.

	p	R^2	Q^2	ρ	out
AB/LogP	0.020	0.87	0.92	-0.26	10,12
AC LogP	0.016	0.72	0.81	-0.43	-
ALOGP	0.006	0.94	0.90	-0.09	9,12
ALOGPs	0.173	0.51	0.94	0.31	6,12
COSMOFrag	0.011	0.92	0.87	0.43	10,12
KowWin	0.006	0.99	0.87	0.66	6,7,12
$\log P$ (o/w)	0.020	0.96	0.72	0.06	6,7,12
miLogP	0.013	0.90	0.85	-0.09	9,12
MLOGP	0.015	0.81	0.64	-0.37	12
SlogP	0.002	0.98	0.19	0.60	9,12
XLOGP2	0.002	0.68	0.72	-0.43	-
XLOGP3	0.035	0.710	0.87	-0.31	9

Unfortunately, it is not possible to validate the above results as experimental $\log P$ values for tetrapyrrolic derivatives of comparable hydrophobicity are lacking, all published values for porphyrins falling within the OECD applicability range [49-54]. However, it is important to note that regression models developed with the PS training set (**6-13**) should fall on the same line the OECD compounds **1-5**. As shown in Figure 3, only COSMOFrag shows a smooth transition between the two data sets.



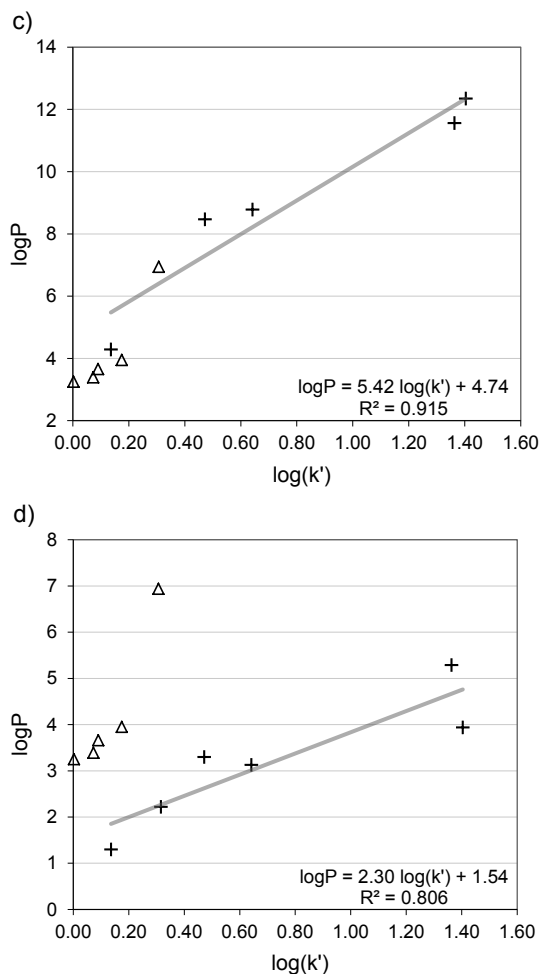


Figure 3. Linear regressions obtained applying AC LogP(a), AB/LogP(b), COSMOFrag(c) and MLOGP(d) prediction models on the training compounds (6-13, represented as + in the plot). Results are compared with OECD prediction (Δ)

Interestingly, departures from linearity are observed when COSMOFrag is applied with more hydrophobic PSs. A sigmoidal trend can be observed that levels off at high $\log(k')$ values (Figure 4a), leading to a correlation coefficient $R^2 = 0.940$. Nevertheless, it is noteworthy that such a sigmoidal function fits perfectly the OECD data points at low $\log(k')$ values (Figure 4b), leading to a correlation coefficient $R^2 = 0.998$ in the OECD range.

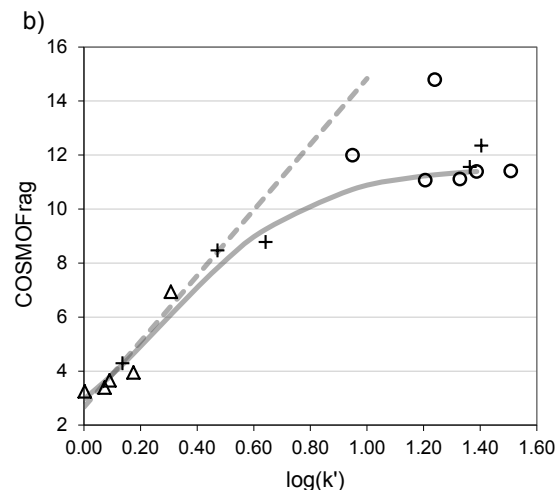
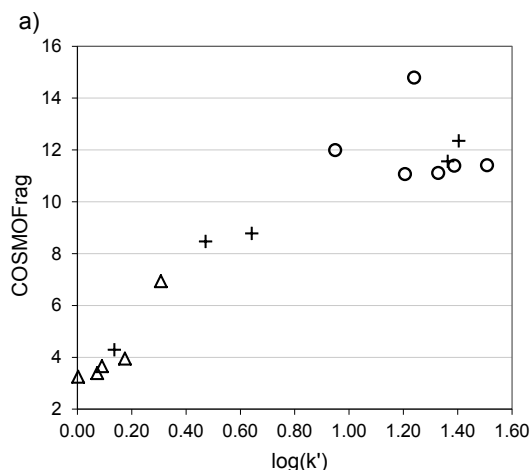


Figure 4. (a) Predicted $\log P$ for OECD (Δ), training (+) and test set (o) according to COSMOFrag method. (b) Comparison between OECD line (dashed line) and the proposed sigmoidal regression (solid line)

Thus among all the tested methods, COSMOFrag seems the best option for predicting the $\log P$ value of highly hydrophobic compounds as it provides a single continuous real function encompassing both the OECD molecules and highly hydrophobic PS. Furthermore, sigmoidal regression (instead of other proposed regression, e.g., polynomial) had a positive derivative in the whole range of measured retention times, reinforcing the notion that molecules with higher $\log P$ values should show also higher $\log(k')$ values.

CONCLUSIONS

A total of 12 commonly available calculation methods (AB/LogP, AC LogP, ALOGP, ALOGPs, COSMOFrag, KowWin, logP (o/w), miLogP, MLOGP, SlogP, XLOGP2 and XLOGP3) have been applied to the prediction of $\log P$ values for highly hydrophobic porphyrin and porphycene derivatives, currently under scrutiny for their use as photosensitizers for photodynamic therapy. Although the lack of experimental $\log P$ values in that range preclude the external validation, the relationship between $\log P$ and $\log(k')$, described in literature for small molecules, was successfully used in order to reduce the problem to a simpler regression analysis. Among all tested methods, COSMOFrag appears as the most suitable to predict the $\log P$ value of highly hydrophobic photosensitizers. Using this method, $\log P$ and $\log(k')$ values are correlated using a sigmoidal-shaped function, maintaining the linear behavior described for small molecules unaltered.

ACKNOWLEDGMENTS

Authors thank Prof. J. Teixidó for his support and Prof. X.Tomás for assistance with the statistical data treatment.

REFERENCES

1. P. Agostinis, K. Berg, K.A. Cengel, T.H. Foster, A.W. Girotti, S.O. Gollnick, S.M. Hahn, M.R. Hamblin, A.

- Juzeniene, D. Kessel, M. Korbelik, J. Moan, P. Mroz, D. Nowis, J. Piette, B.C. Wilson, J. Golab, Photodynamic therapy of cancer: An update, *CA: A Cancer Journal for Clinicians*, 61:250–281, **2011**.
2. T.N. Demidova, M.R. Hamblin, Photodynamic Therapy Targeted to Pathogens, *Int J Immunopathol Pharmacol.* 17(3): 245–254, **2004**.
 3. S. Anand, B.J. Ortel, S.P. Pereira, T. Hasan, E.V. Maytin, Biomodulatory approaches to photodynamic therapy of solid tumors, *Cancer Lett.* 326(1): 8-16, **2012**.
 4. Y.Lee, E.D. Baron, Photodynamic Therapy: Current Evidence and Applications in Dermatology, *Semin. Cutan. Med. Surg.*, 30(4):199-209, **2011**.
 5. C.A. Robertson, D. Hawkins, H. Abrahamse. Photodynamic therapy (PDT): A short review on cellular mechanisms and cancer research applications for PDT. *J. Photochem. Photobiol. B*, 96:1–8, **2009**.
 6. E.S. Nyman, P.H. Hynninen. Research advances in the use of tetrapyrrolic photosensitizers for photodynamic therapy. *J. Photochem. Photobiol. B*, 73:1–28, **2004**.
 7. N.L. Oleinick, R.L. Morris, I. Belichenko. The role of apoptosis in response to photodynamic therapy: what, where, why and how. *Photochem. Photobiol. Sci.*, 1:1–21, **2002**.
 8. A. Castano, T.Demidova, M.Hamblin. Mechanisms in photodynamic therapy: Part three-photosensitizer pharmacokinetics, biodistribution, tumor localization and modes of tumor destruction. *Photodiagnosis and Photodynamic Therapy*, 2(2):91–106, **2005**.
 9. J.C. Stockert, M. Cañete, A. Juarranz, A. Villanueva, R.W. Horobin, J.I. Borrell, J. Teixidó, S. Nonell. Porphycenes: Facts and prospects in photodynamic therapy of cancer. *Curr. Med. Chem.*, 14(9):997-1026, **2007**.
 10. C. Richert, J.M.Wessels, M.Müller, M. Kisters, T. Benninghaus, A.E. Goetz. Photodynamic antitumor agents: β -methoxyethyl groups give access to functionalized porphycenes and enhance cellular uptake and activity. *J.Med. Chem.*, 37:2797–2807, **1994**.
 11. J. Moan, K. Berg, E. Kwam, A. Western, Z. Malik, A. Rück, H. Schneckenburger. Intracellular localization of photosensitizers. *Ciba Found. Symp.*, 146:95–111, **1989**.
 12. D. Kessel, The role of subcellular localization in initiation of apoptosis by photodynamic therapy. *Photochem. Photobiol.*, 65: 422-426, **1997**.
 13. D. Kessel, Correlation between subcellular localization and photodynamic efficacy. *J. Porphyrins Phtalocyanines.*, 8: 1009-1014, **2004**.
 14. S.Wildman, G. Crippen. Prediction of physicochemical parameters by atomic contributions. *J. Chem. Inf. Comput. Sci.*, 39:868–873, 1999.
 15. K.Woodburn, N.J. Vardaxis, J.S.Hill, A.H. Kaye,D.R. Phillips. Subcellular localization of porphyrins using confocal laser scanning microscopy. *Photochem. Photobiol.*, 54(5):725–732, 1991.
 16. L. Rao, D. Perez, E. White. Lamin proteolysis facilitates nuclear events during apoptosis. *J. Cell Biol.*, 135(6):1441–1455, 1996.
 17. P.Margaron, M. Grégoire, V. Scasnar, H. Ali, J.E. Lier. Structure-photodynamic activity relationships of a series of 4-substituted zinc phthalocyanines. *Photochem. Photobiol.*, 63(2):217–223, **1996**.
 18. B.W. Henderson, D.A. Bellnier, W.R. Greco, A. Sharma, R.K. Pandey, L.A. Vaughan, K.R. Weishaupt, T.J. Dougherty. An in vivo quantitative structure-activity relationship for a congeneric series of pyropheophorbide derivatives as photosensitizers for photodynamic therapy. *Cancer Res.*, 57:4000–4007, 1997.
 19. R. Vanyúr, K. Héberger, I. Kövesdi, J. Jakus. Prediction of tumoricidal activity and accumulation of photosensitizers in photodynamic therapy using multiple linear regression and artificial neural networks. *Photochem. Photobiol.*, 75(5):471–478, 2002.
 20. P. Gramatica, E. Papa, S. Banfi, E. Caruso. QSAR Modeling and Prediction of Tumoricidal Activity of Aryl-Porphyrins in Photodynamic Therapy, 11th Congress of the European Society for Photobiology, Aix-les-Bains (France), 2005.
 21. C.P. Brangwynne, G.H. Koenderink, F.C. MacKintosh, D.A. Weitz. Cytoplasmic diffusion: molecular motors mix it up. *J. Cell. Biol.*, 183(4):583–587, 2008.
 22. Y.Huang, P. Mroz, T. Zhiyentayev, S.K. Sharma, T. Balasubramanian, C. Ruzié, M. Krayer, D. Fan, K.E. Borbas, E. Yang, H.L. Kee, C. Kirmaier, J.R. Diers, D.F. Bocian, D. Holten, J.S. Lindsay, M. Hamblin. In vitro photodynamic therapy and quantitative structure-activity relationship studies with stable synthetic near-infrared-absorbing bacteriochlorin photosensitizers. *J.Med. Chem.*, 53(10):4018-4027, **2010**.
 23. R.Tejedor-Estrada, S.Nonell, J.Teixidó, M.Li.Sagristá, M.Mora, A.Villanueva, M.Cañete, J.C.Stockert, An artificial neural network model for predicting the subcellular localization of photosensitizers for photodynamic therapy of solid tumors, *Curr. Med. Chem.*, 19, 2472-2482, **2012**.
 24. G. Li, A. Graham, Y. Chen, M.P. Dobhal, J. Morgan, G. Zheng, A. Kozyrev, A. Oseroff, T.J. Dougherty, R.K. Pandey. Synthesis, comparative photosensitizing efficacy, human serum albumin (site II) binding ability, and intracellular localization characteristics of novel benzobacteriochlorins derived from vic-dihydroxybacteriochlorins. *J. Med. Chem.*, 46:5349–5359, **2003**.
 25. T. Cheng, Y. Zhao, X. Li, F. Lin, Y. Xu, X. Zhang, Y. Li, R. Wang, L. Lai. Computation of octanol-water partition coefficients by guiding an additive model with knowledge. *J. Chem. Inf. Model.*, 47(6):2140–2148, **2007**.
 26. C. Hansch, A. Leo. Exploring QSAR. Fundamentals and Applications in Chemistry and Biology. ACS Professional Reference Book. American Chemical Society, Washington, **1995**.
 27. R. Todeschini, V. Consonni. Handbook of Molecular Descriptors. Wiley-VCH, Weinheim, Germany, **2000**.
 28. T. Fujita, J. Iwasa, C. Hansch, A new substituent constant derived from partition coefficients. *J. Am. Chem. Soc.*, 86:5175–5180, **1964**.
 29. P. Broto, G. Moreau, C. Vandycke. Molecular structures: Perception, autocorrelation descriptor and SAR studies. *Eur. J. Med. Chem.*, 19:71–78, **1984**.
 30. Inc. Chemical Computing Group. Molecular operating environment (MOE), v.2007.09, **2007**.
 31. V.N. Viswanadhan, A.K. Ghose, G.R. Revankar, R.K. Robins. Atomic physicochemical parameters for three dimensional structure directed quantitative structure-activity relationships. 4. Additional parameters for hydrophobic and dispersive interactions and their application for an automated superposition of certain

- naturally occurring nucleoside antibiotics. *J. Chem. Inf. Comput. Sci.*, 29(3):163–172, **1989**.
32. I.V. Tetko, G.I. Poda. Prediction of logP with property-based methods. Drug Properties-Measurement and Prediction. Wiley-VCH, Weinheim, Germany, **2008**.
 33. Y. Sakuratani, K. Kasai, Y. Noguchi, J. Yamada. Comparison of predictivities of logP calculation models based on experimental data for 134 simple organic compounds. *QSAR Comb. Sci.*, 26(1):109–116, **2007**.
 34. I.V. Tetko, V.Y. Tanchuk, A.E. Villa. Prediction of n-octanol/water partition coefficients from PHYSPROP database using artificial neural networks and e-state indices. *J. Chem. Inf. Comput. Sci.*, 41(5):1407–1421, **2001**.
 35. G. Kellogg, D. Abraham. Hydrophobicity: is logP(o/w) more than the sum of its parts? *Eur. J. Med. Chem.*, 35:651–661, **2000**.
 36. S. Ben-Dror, I. Bronshtein, A. Wiehe, B. Röder, M.O. Senge, B. Ehrenberg. On the correlation between hydrophobicity, liposome binding and cellular uptake of porphyrin sensitizers. *Photochem. Photobiol.*, 82:695–701, **2006**.
 37. A. Sholto, B. Ehrenberg. Hydrophobicity, topography in membranes and photosensitization of silicon phthalocyanines with axial ligands of varying lengths. *Photochem. Photobiol. Sci.*, 7(3):344–351, **2008**.
 38. I.V. Tetko, J. Gasteiger, R. Todeschini, A. Mauri, D. Livingstone, P. Ertl, V.A. Paluyulin, E.V. Radchenko, N.S. Zefirov, A.S. Makarenko, V.Y. Tanchuk, V.V. Prokopenko. Virtual computational chemistry laboratory - design and description. *J. Comput. Aid. Mol. Des.*, 19:453–463, **2005**.
 39. Virtual Computational Chemistry Laboratory. VCCLAB, <http://www.vcclab.org>, **2005**.
 40. S.A. Wildman, G.M. Crippen. Prediction of Physicochemical Parameters by Atomic Contributions. *J. Chem. Inf. Comput. Sci.*, 39(5): 868–873, **1999**.
 41. I. Moriguci, S. Hirono, Q. Liu, I. Nakagome, Y. Matsushita. Simple Method of Calculating Octanol/Water Partition Coefficient, *Chem. Pharm. Bull.*, 40(1):127–130, **1992**.
 42. OSIRIS Property Explorer, Actelion Pharmaceuticals Ltd, Gewerbestrasse 16, 4123 Allschwil, Switzerland.
 43. R. Mannhold, Lipophilicity: Its Calculation and Application in ADMET Predictions, *Virtual ADMET Assessment in Target Selection and Maturation*, B. Testa and L. Turski (Ed.), IOS Press, Amsterdam, **2006**.
 44. W.M. Meylan, P.H. Howard, Estimating logP with atom/fragments and water solubility with log P, *Perspect. Drug. Discov. Des.*, 19(1):67–84, **2000**.
 45. A.K. Ghose, .N. Viswanadhan, J.J. Wendoloski, Prediction of hydrophobic (lipophilic) properties of small organic molecules using fragmental methods: an analysis of ALOGP and CLOGP methods, *J. Phys. Chem. A*, 102(21):3762–3772, **1998**.
 46. I.V. Tetko, G.I. Poda, Application of ALOGPS 2.1 to predict logP distribution coefficient for Pfizer Proprietary Compounds, *J. Med. Chem.*, 47(23):5601–5604, **2004**.
 47. OECD Guide line for Testing of Chemicals. Partition coefficient (n-octanol/water), high performance liquid chromatography (HPLC) method. *Council on 30th-March*, 117, **1989**.
 48. R. Put, Y. Van der Heyden. Review on modelling aspects in reversed-phase liquid chromatographic quantitative structure-retention relationships. *Anal. Chim. Acta*, 602(2):164–172, **2007**.
 49. G. Meng, B.R. James, M. Korbelik, K.A. Skov. Porphyrin chemistry pertaining to the design of anticancer drugs. Part 2, the synthesis and in vitro tests of water-soluble porphyrins containing, in the meso positions, the functional groups: 4-mehtylpyridinium, or 4-sulfonatophenyl, in combination with phenyl, 4-pyridyl, 4-nitrophenyl, or 4-aminophenyl. *Cancer J. Chem.*, 72:2447–2457, **1994**.
 50. C. Drain, X. Gong, V. Ruta, C. Soll, P. Chiccoineau. Combinatorial synthesis and modification of functional porphyrin libraries; identification of new, amphipathic motifs for biomolecule binding. *J. Comb. Chem.*, 1(4):286–290, **1991**.
 51. H. Li, Z. Cao, H. Xiao. Synthesis of lactosylated piperazine porphyrins and their hepatocyteselective targeting. *Med. Chem. Res.*, 16:28–38, **2007**.
 52. E. Milanesio, G. Alvarez, S. Bertolotti, E. Durantini. Photophysical characterization and photodynamic activity of metallo 5-(4-(trimethylammonium)phenyl)-10, 15,20-tris(2,4,6- trimethoxyphenyl)porphyrin in homogeneous and biomimetic media. *Photochem. Photobiol. Sci.*, 7:963–972, **2008**.
 53. D. Lazzeri, M. Rovera, L. Pascual, E. Durantini. Photodynamic studies and photoinactivation of Escherichia Coli using meso-substituted cationic porphyrin derivatives with assymetric charge distribution. *Photochem. Photobiol.*, 80:286–293, **2004**.
 54. M. Kepczynski, R. Pandian, K. Smith, B. Ehrenberg. Do liposome-binding constants of porphyrins correlate with their measured and predicted partitionig between octanol and water? *Photochem. Photobiol.*, 76(2):127–134, **2002**.